

Laser sensors—gas analyzers based on smart waveguide CO₂ lasers and resonance photoacoustic detectors and their applications

A.I. Karapuzikov,¹ I.V. Sherstov,¹ B.G. Ageev,²
V.A. Kapitanov,² and Yu.N. Ponomarev²

¹ *Institute of Laser Physics,
Siberian Branch of the Russian Academy of Sciences, Novosibirsk*

² *Institute of Atmospheric Optics,
Siberian Branch of the Russian Academy of Sciences, Tomsk*

Received February 2, 2007

We present an overview of the main results of long-term collaboration between the Institute of Atmospheric Optics and the Institute of Laser Physics in development and design of a series of laser sensors—gas analyzers based on differential resonance photoacoustic detectors and a waveguide continuous-wave (CW) CO₂ laser with the computer-controlled wavelength tuning. Basic elements of the gas analyzers and their characteristics are described along with examples of application to analysis of molecular compounds in air and biosphere—atmosphere exchange processes.

Introduction

Rapid development of methods of laser gas analysis is caused by the advent of new lasers and improvement of existing lasers with continuous or discrete wavelength tuning performed automatically with the aid of a computer or specialized processor. Another decisive factor is the progress in development of methods of recording very weak selective absorption with the use of small-size multipass gas cells,¹ including high-Q cavities,² or with the high-sensitivity photoacoustic detectors.^{3,4} The method of laser photoacoustic analysis of gas media is one of the most promising due to its simplicity, reliability, high sensitivity, and relatively low cost. In combination with smart IR lasers, such as CW CO₂ or CO lasers or diode lasers, the photoacoustic detection technique provides for the measurement of the concentration of many chemical compounds in multicomponent gas mixtures and in the atmosphere at the level from ppm to ppt as low.^{4,5}

This paper is a review of the main results of the long-term cooperation between the Institute of Atmospheric Optics and the Institute of Laser Physics in development of high-sensitivity laser photoacoustic sensors and gas analyzers for various scientific and environmental applications.

1. Basic components of laser sensors—gas analyzers

1.1. Continuous-wave tunable waveguide CO₂ laser

For many years the development and design of CW tunable waveguide CO₂ lasers for gas analyzers

has been a priority research field at the Institute of Laser Physics. The most successful laser models were called smart, because all operations of tuning and stabilization of radiation parameters in these lasers are performed automatically following a computer program.

Waveguide CO₂ lasers are characterized by small size compared to CO₂ lasers of other types and by the high gain necessary to achieve lasing at weak lines and to provide a wider tuning range. The use of high-frequency (HF) excitation of CO₂ lasers allows one to overcome the problems associated with the presence of high-voltage power supplies and to reduce the discharge noise.⁶

The sensors and gas analyzers described below employed HF-excited waveguide CO₂ laser with a metal-ceramic waveguide of a square cross section. The laser housing is made from an Ø88×650 mm stainless steel tube. The tube serves a vacuum jacket and a frame for the optical cavity. Flanges are welded at both ends of the tube, and the optical elements of the cavity are installed on them with vacuum seals. This design features high stiffness and is insensitive to external mechanical impacts.

The 2.2×2.2×450 mm metal-ceramic waveguide is formed by two plane oxidized aluminum electrodes and two plane polished leucosapphire plates. As the HF voltage is applied to the upper electrode, the capacitive discharge is initiated in the waveguide, and this discharge is used to excite the laser gas medium. The presence of a waveguide in a laser increases the coefficient of usage of the active volume. However, in some cases the modal selectivity decreases, which requires the selection of the proper optical arrangement of the cavity.

Figure 1 shows the optical arrangement of a tunable waveguide laser with the cavity described in

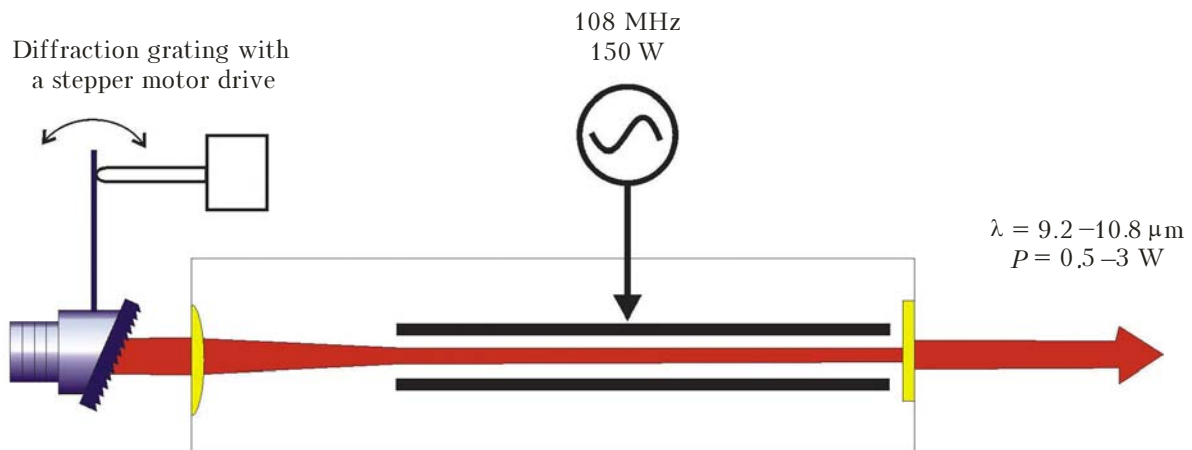


Fig. 1. Optical arrangement of a tunable waveguide CO₂ laser with HF excitation.

Refs. 7 and 8. The radiation exits through a plane window with the transmission coefficient of 4%. The totally reflecting back spherical mirror is formed by a combination of antireflection plano-convex lens from ZnSe and a plane reflecting diffraction grating operating in the autocollimation mode.

A gold-coated diffraction grating with a period of 150 mm^{-1} is mounted in a rigid lever-type turning unit. The grating was turned by a precision linear pusher driven by a stepper motor. The linear pusher had built-in sensors of the initial and final positions, due to which the turning unit allowed a required angular position of the diffraction grating to be set with high accuracy and repeatability, as the laser was tuned over the lasing lines.

The study of the spectral composition of radiation of such lasers has shown that at strong lasing lines, especially, in the $10\text{-}\mu\text{m}$ region, the radiation included parasitic mode beats at frequencies from several to 20–40 MHz. The appearance of these beats is attributed to some minor difference of the waveguide cross section from a square, which is usually present in actual waveguide lasers.

To control mode beats, selective losses in the laser were increased through the use of lenses with different focal lengths. Experiments have shown that at $f_1 > 410 \text{ mm}$ mode beats were not observed in any lasing line at all.

The radiation intensity distribution over the cross section in the far zone took Gaussian profile, that is, the laser operated at the lowest EH_{11} waveguide mode. The total divergence of the beam at wavelengths of 9.2 and $10.6 \mu\text{m}$ was respectively 8.8 and 9.4 mrad. The laser emitted at more than 70 lines with the output power up to 2.5–3 W at strong lines and up to 0.3–0.5 W at weak lines. The wavelength tuning was carried out automatically according to an individual calibration table for every laser. The main parameters of the designed tunable waveguide CO₂ laser are tabulated below.

Operating mode	Continuous-wave, repetitively pulsed
Spectral region, μm :	
– for $^{12}\text{C}^{16}\text{O}_2$	9.2–10.8
– for $^{13}\text{C}^{16}\text{O}_2$	9.6–11.4
Output power, W:	
– at strong lines	2.5–3
– at weak lines	> 0.5
Number of lasing lines (for $^{12}\text{C}^{16}\text{O}_2$)	> 60
Mode structure of radiation	Single mode, single frequency
Polarization	Linear
Output beam diameter, mm	2
Divergence (total, e^{-2}), mrad	8.8–9.4
Excitation of active medium, MHz	HF discharge, 108
Power of HF pump generator, W	150
Cooling (radiator + HF generator)	water cooling, 2 L/min
Power supply/consumed power	+24 V/400 V · A
Overall dimensions, mm	
– radiator	840 × 90 × 150
– HF pump generator	433 × 100 × 42
Mass, kg	
– radiator	10
– HF pump generator	3

1.2. Differential photoacoustic cell based on a Helmholtz cavity

The basic scheme of a photoacoustic detector (PAD) based on the ring differential Helmholtz cavity (DHC)⁹ is shown in Fig. 2. The ring cavity consists of two identical cylindrical channels connected at the ends by identical cavities. A microphone is mounted at the center of a lateral wall of every channel. The connecting cavities are closed by transparent windows. A characteristic feature of this cavity, as well as other DHCs,¹⁰ is that at the repetitively pulsed irradiation of one of its channels at a resonance frequency in the presence of an absorbing gas the standing acoustic wave is formed with the resonance frequency

$$f = v/2L,$$

where v is the speed of sound, L is the channel length.

At a resonance frequency, antinodes of pressure oscillations are located at the center of the channels, while nodes are located near windows, and the pressure oscillations in the different channels are in antiphase, as well as in DHC.

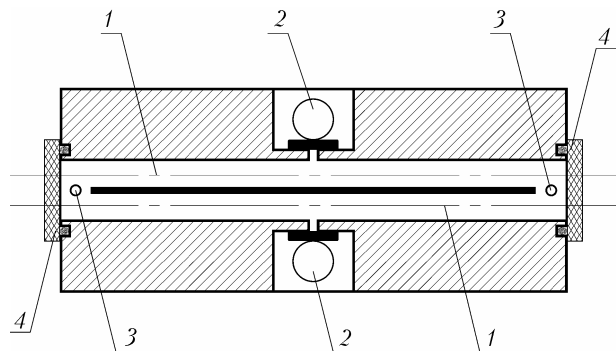


Fig. 2. Block diagram of the ring differential resonance photoacoustic detector of the flow-through type: acoustic cavity 1; microphone 2; gas inlet-outlet 3; window 4.

This circumstance allows the differential scheme of measurements to be used. In this case, electric signals from microphones set in different PAD channels are entered in the differential amplifier. As a result, the useful (antiphase) signal is doubled, while inphase signals (noise of air blow through PAD, external acoustic noise, vibration, etc.) are efficiently suppressed. The cavities connecting the channels near windows can be made as cylindrical hollows of 10 ... 20% depth.

In developing prototype laser sensors and gas analyzers, we have made and tested several models of ring differential PAD. For the real-time measurement of the concentration of foreign gases, PAD the air sample is permanently pumped through the device. A gas inflow into PAD and outflow were carried out through holes located in the connecting cavities near the detector windows, where the nodes of pressure oscillations at the PAD resonance frequency lie. The contribution from noise introduced by the gas inflow-outflow was thus minimized.

As the airflow rate varied from 0 to 1.2 l/min, the acoustic noise remained at the minimum level. At the flow rate higher than 1.4 l/min, the noise increased sharply, which is connected with the transition of the gas flow from the laminar mode to the turbulent mode. The PAD response time is determined by the time of delivery of the air sample. When the sampling hose ($\varnothing 2$ mm, length ~ 1.5 m) was used and the flow rate was 0.6 l/min, the PAD response time was ~ 1 s and decreased as the hose length decreased.

The ring differential PAD was calibrated against the known absorption of gaseous CO_2 or SF_6 and the minimum detected absorption coefficient and the threshold sensitivity were determined. The PAD characteristics are tabulated below.

Dimensions of PAD cavities, mm	$\varnothing 6 \times 90$
Dimensions of connecting caves, mm	$\varnothing 17 \times 8$
Beam diameter at PAD center, mm	1.54 (at e^{-2} level)
Background acoustic noise, $\mu\text{V} / \text{Hz}^{1/2}$	0.24
Background photoacoustic signal, $\mu\text{V}/\text{W}$	4.7
Resonance frequency, Hz	1768
Figure of merit	23 (at 0.5 level)
PAD constant, $\text{V}/\text{cm}^{-1} \cdot \text{W}$	12.9
Threshold sensitivity, $\text{cm}^{-1} \cdot \text{W} \cdot \text{Hz}^{-1/2}$	$2.4 \cdot 10^{-9}$
Minimum detected absorption, cm^{-1}	$7.5 \cdot 10^{-10}$

The minimum absorption detected with the use of the CO_2 laser and resonance PAD with a longitudinal cavity is $\sim 10^{-9} \text{ cm}^{-1}$ for the case that PAD is outside the laser cavity,³ but if PAD is placed inside the laser cavity, it achieves $1.8 \cdot 10^{-10}$ (see Ref. 11) and $3.3 \cdot 10^{-10} \text{ cm}^{-1}$ (see Ref. 12).

2. Prototype gas-analysis devices based on a waveguide CO_2 laser and differential PAD

2.1. Laser PA leak detector

The operation of this leak detector is based on the detection of leakages of a gas marker through microcracks or seams. The leak detector consists of an air-cooled waveguide CO_2 laser with HF excitation, a photoacoustic detector, a power meter, an air pump, and a controller. The leak detector works from a +12 V DC power supply or from an electric battery, which allows the leak detector to be operated as a stand-alone device under various conditions, in particular, under field conditions.

The laser operates in the repetitively pulsed mode with the pulse repetition frequency coinciding with the lowest PAD resonance frequency. The lasing line is selected according to the type of the gas marker.

The sensitivity of the leak detector has been measured against a calibrated leakage of $1 \cdot 10^{-5} \text{ Pa} \cdot \text{m}^3/\text{s}$ intensity of the gas mixture of $\text{N}_2 + 20 \text{ ppm SF}_6$. In a series of experiments with a flow rate of 0.6 l/min, PAD signals were measured with the total interception of nitrogen with SF_6 admixture flowing out from the calibrated leak, as well as in ordinary air blown through PAD (that is, background signal). The sensitivity of the designed leak detector measured in this way amounted to $1 \cdot 10^{-10} \text{ Pa} \cdot \text{m}^3/\text{s}$ as recalculated to the SF_6 concentration.

A "Karat" laser photoacoustic leak detector¹³ (Fig. 3) is made as a portable device with a remote control. The remote control is equipped with a telescopic sampler and a light indicator of the signal level. It is connected with the leak detector by a thin hose and an electric cable. The remote control is used to turn the leak detector on/off. In addition, it indicates the concentration of the gas marker. It is also possible to display the power of laser radiation.



Fig. 3. Appearance of a “Karat” laser photoacoustic leak detector.

The leak detector can be connected to a computer through a USB port on the front panel. It can be controlled both using the remote control and a computer independently. The control program not only starts and stops the leak detector, but also allows the time dynamics of the gas marker concentration in a sample to be displayed. Specifications of the “Karat” leak detector are tabulated below.

Type of detector	PAD
Source of radiation	CO ₂ laser
Radiation wavelength, μm	10.6
Mean output power, W, no higher than	1
Cooling	Air cooling
Gas marker used	SF ₆
Sensitivity to SF ₆ leak, Pa · m ³ /s	$1 \cdot 10^{-10}$
Concentration of the gas marker in carrier gas, %	0.01–0.1
Flow rate of air sample, l/min, no higher than	1
Connection to a computer	USB port
Availability for service, min, no longer than	0.5
Supply voltage, V	+12 DC (battery)
Consumed power, W, no higher than	30
Service life before the battery recharge (7 A · h), h, no shorter than	2
Overall dimensions, mm, no larger than:	
– leak detector	470 × 193 × 108
– remote control	240 × 53 × 25
– length of the telescopic sampler	147–900
Mass, kg, no larger than:	
– leak detector	5.5
– remote control	0.15

The “Karat” detector features far higher sensitivity compared to commercial He leak detectors in the backflow mode and compared to halogen leak detectors. Its mass and dimensions are comparable with those of halogen detectors. It can be operated from an electric battery and has low power consumption. The time of “Karat” availability for service is shorter than 1 min. In addition, the

“Karat” leak detector reacts to the presence of other gases, in particular, household gas (propane, butane), alcohol, acetone, and ethylene vapor in air, which gives additional capabilities of detecting the leaks of these gases.

In the process of leak detection, the laser leak detector sucks in an air sample with the gas marker admixture from the area near the leak with the remote telescopic probe. Due to the high mass, the diffusion rate of SF₆ molecules in air is low, and therefore they are located near a leak, which facilitates the detection. The autonomous power supply and the backpack design make the “Karat” detector a convenient device in the case of long gas distribution pipelines.

2.2. Multiwave laser gas analyzers

2.2.1. Laser gas analyzer with an external PAD (LGA-1)

The LGA-1 appearance is shown in Fig. 4. This gas analyzer employs a waveguide CO₂ laser with the fast discrete wavelength tuning in a range from 9.3 to 10.9 μm . The active medium of the laser can be ¹²CO₂ and ¹³CO₂. This allows the lasing at 150 wavelengths to be obtained. High-sensitivity flow-through PAD with the corresponding software and the computer data processing allows small absorption coefficients $\sim 10^{-9} \text{ cm}^{-1}$ to be measured in the volume of an analyzed sample of 10 cm³.

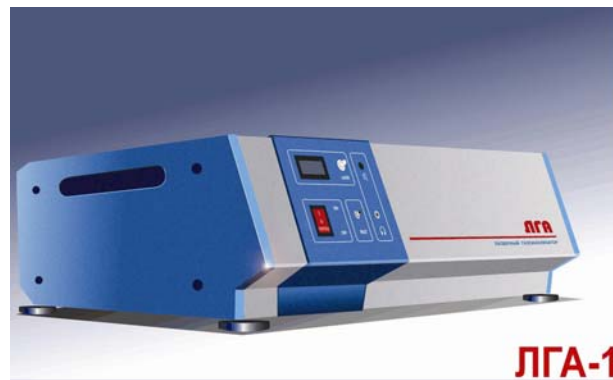


Fig. 4. Appearance of a laser gas analyzer with an external PAD.

Applications of LGA-1:

- measurements of concentrations of atmospheric and anthropogenic gases (C₂H₄, NH₃, O₃, C₆H₆, SO₂, SF₆, N₂O, CH₃F, CH₃C, etc.) at the ppm down to ppb level;
- monitoring of concentrations of chemical molecular compounds in gases, including toxic ones, in the atmosphere and technological processes;
- analysis of absorption spectra of expired air and determination of gas markers of various diseases.

LGA-1 can be adapted to the operation with other types of molecular lasers, such as CO₂, ammonia, and hydrogen fluoride lasers.

2.2.2. Laser gas analyzer with a photoacoustic detector

A resonance PAD of the differential type is installed inside a high-Q cavity of a CO₂ laser (Fig. 5). In contrast to Ref. 14, in our case the laser and PAD make up an all-in-one robust construction, due to which the number of intracavity elements is minimized. This allows the power of the optical radiation inside the cavity and the passive stability of the optical cavity to be increased. The design of this gas analyzer is protected by patent of the RF.⁹



Fig. 5. Appearance of a laser gas analyzer with an intracavity PAD.

The block diagram of a gas analyzer with an intracavity PAD is shown in Fig. 6.

The cavity of a waveguide laser houses PAD 1, whose body is a part of the construction of the optical cavity. It is fastened mechanically to the laser

active element and to the wavelength-tuning unit. The laser active volume and PAD acoustic channels are sealed with the use of lens 14 and the output window 6. All vacuum seals are made with the use of rings 7. The lens is necessary to reduce differential losses and to improve the selectivity of the cavity. The output window separates the active volume of the emitter and the PAD volume. Both intracavity optical elements 14 and 6 have antireflection coating in the range of laser wavelength tuning.

Such a packaging of the laser and PAD ensures the construction robustness at the minimum number of intracavity optical elements, which allows us to minimize the losses, to reduce fluctuations, and to increase the radiation power, thus increasing the threshold sensitivity of the gas analyzer to the level of $2.4 \cdot 10^{-9} \text{ W} \cdot \text{cm}^{-1} \cdot \text{Hz}^{-1/2}$. Another way to increase the power of radiation inside the cavity is to use the repetitive pulsed pumping of the laser active medium with the higher power of HF pump pulses, keeping the mean power unchanged. No such a possibility exists in lasers with the repetitively pulsed mode obtained with the aid of a mechanical modulator.¹⁴ The investigations of the spectrum of laser emission with built-in PAD have shown the presence of about 60 lines for the basic isotopic modification of the CO₂ molecule.

3. Some applications of laser PA sensors—gas analyzers

3.1. Investigation of plant gas exchange kinetics

To solve some problems in plant ecology, physiology, and cultivation, it is necessary to know

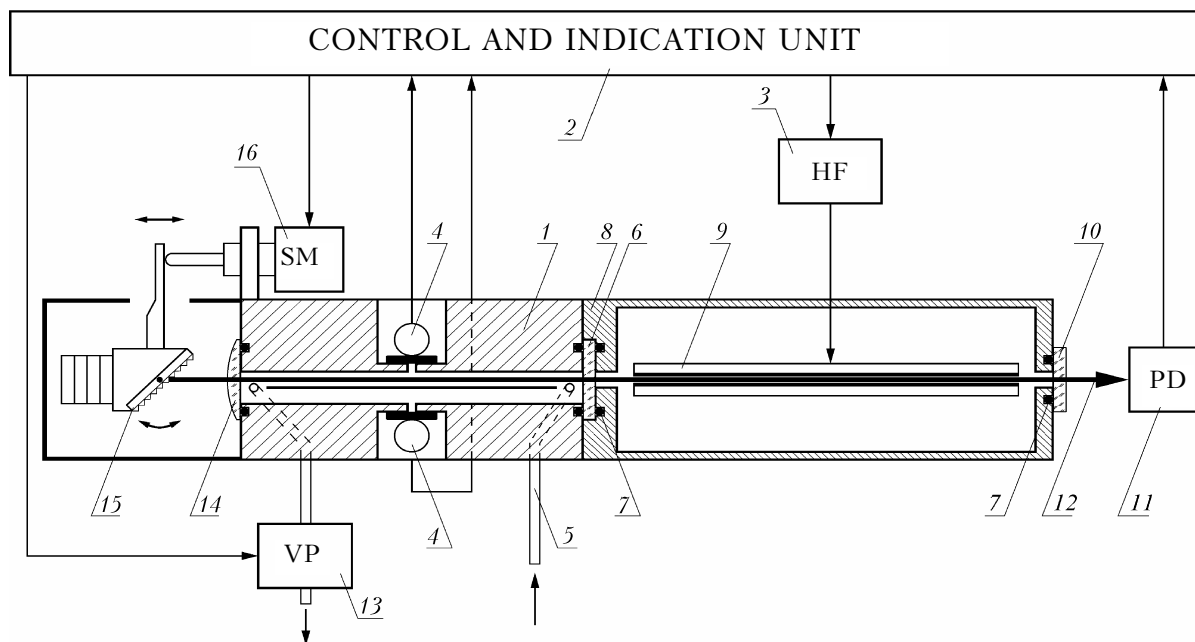


Fig. 6. Block diagram of a gas analyzer based on a tunable waveguide CO₂ laser with HF excitation and intracavity PAD: flow-through photoacoustic detector 1; control and display unit 2; HF pump generator 3; microphone 4; PAD gas inflow and outflow 5; window 6; seal 7; active element of CO₂ laser 8; waveguide 9; output mirror 10; photodetector 11; laser beam 12; vacuum pump 13; lens 14; diffraction grating 15; stepper motor 16.

gas exchange processes, regularities of their variation at one or another change in the environmental conditions. The method most widely used to study the gas exchange in plants is the infrared (IR) optical gas analysis in particular, laser PA gas analysis with CO and CO₂ lasers.¹⁵ The gas analysis technique described above was used to study the dark respiration of the leaf apparatus of herbaceous and arborous plants. Figure 7a shows the absorption spectrum of a gas sample obtained at the dark respiration of Siberian pine needles along with the previously recorded spectrum of the control gas mixture CO₂-N₂ (CO₂ concentration of 5000 ppm) and the indoor air. In the spectrum, one can clearly see two peaks corresponding to the emission of carbon dioxide (944.194 cm⁻¹), which is the main component of the gas-exchange cycle, and ethylene (949.479 cm⁻¹), being the gaseous plant hormone. It is synthesized in plants, regulates their growth and fruit ripening, and characterizes the plant response to various stress factors.

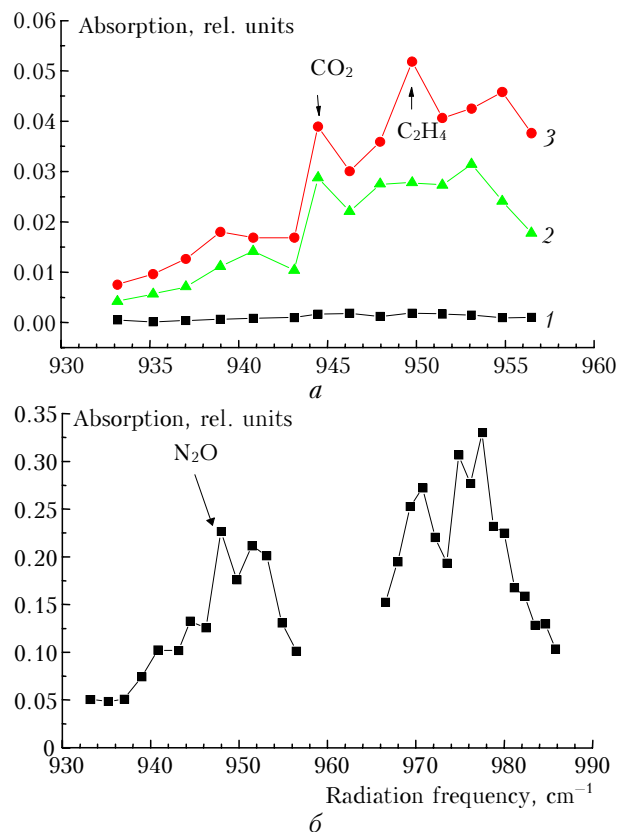


Fig. 7. Demonstration of application of laser PA gas analyzers with waveguide CO₂ lasers: (a) absorption spectra of gases in the range of a CO₂ laser (*P*-branch of the 10 μm band): indoor air 1; fur tree needle emission 2; control mixture 3; (b) histogram of the spectrum of expired air sampled from a bronchial asthma patient.

The emission of ethylene by fruits demonstrates the obvious growth during the ripening and reaches maximum, when a fruit is at the state of highest ripeness. In this connection, we have checked

experimentally that ethylene is the main gas emitted by ripe fruits of fruit trees, while no other components are present in comparable amounts.

3.2. Detection of marker gases in expired air

Under normal conditions, the expired air contains about 400 volatile compounds. Some compounds, for example CO₂, N₂, O₂, and H₂O vapor, are present, in a certain proportion, in the expired air of all people, while the increased concentration of other substances absorbing at CO₂ laser lines may be indicator of a disease or some stress. To test the capabilities of the laser PA analysis in medical diagnostics with the use of laser gas analyzer with intracavity PAD, we have carried out a cycle of measurements of the composition of expired air in people of the control group (healthy people) and experimental group (patients). The combined analysis of experimental data and questioning results has been performed. As a result, the possibility of recording gas markers such as N₂O, C₂H₄, and H₂O₂ in patients with certain diseases has been demonstrated. As an example, Figure 7b shows a scan of a sample of expired air of a bronchial asthma patient with a characteristic peak corresponding to the N₂O absorption (948 cm⁻¹).

References

1. A. Nadezhdinskii, A. Berezin, S. Chernin, O. Ershov, and K.V. Kutnya, *Spectrochim. Acta, Part A* **55**, 2083–2089 (1999).
2. D. Romanini, A.A. Kachanov, N. Sadeghi, and F. Stoekel, *Chem. Phys. Lett.* **264**, 316–322 (1997).
3. A. Miklos and P. Hess, *Rev. Sci. Instrum.* **72**, No. 4, 1937–1955 (2001).
4. I.G. Calasso, V. Funtov, and M.W. Sigrist, *Appl. Opt.* **36**, No. 15, 3212–3216 (1997).
5. S. Schilt, L. Thevenaz, M. Nikles, K. Emmenegger, and C. Huglin, *Spectrochim. Acta, Part A* **60**, 3259–3268 (2004).
6. U.E. Hochuli and P.R. Haldemann, *Rev. Sci. Instrum.* **57**, No. 9, 2238–2241 (1986).
7. R. Abrams, *IEEE J. Quantum* **8**, No. 11, 838–843 (1972).
8. J.J. Degnan, *Appl. Phys. J.*, No. 11, 1–33 (1976).
9. V.A. Kapitanov, A.I. Karapuzikov, Yu.N. Ponomarev, and I.V. Sherstov, “*Resonance Photoacoustic Detector and Photoacoustic Laser Gas Analyzer*,” RF Patent No. 1746 (2006).
10. Yu.N. Ponomarev, B.G. Ageev, M.W. Sigrist, V.A. Kapitanov, D. Courtois, and O.Yu. Nikiforova, *Laser Photoacoustic Spectroscopy of Intermolecular Interactions in Gases* (RASKO, Tomsk, 2000), 200 pp.
11. F.J.M. Harren, F.G.C. Bijnen, J. Reuss, L.A.C.J. Voeselek, and C.W.P.M. Blom, *Appl. Phys. B* **50**, 137–144 (1990).
12. T. Fink, S. Buscher, R. Gabler, A. Dax, and W. Urban, *Rev. Sci. Instrum.* **67**, No. 11, 4000–4004 (1996).
13. V.A. Kapitanov, A.I. Karapuzikov, Yu.N. Ponomarev, and I.V. Sherstov, “*Photoacoustic Laser Leakage Detector*,” RF Patent No. 38228 (2004).
14. L.S. Rothman, D. Jacquemart, A. Barbe, C.D. Benner, and M. Birk, *J. Quant. Spectrosc. & Radiat. Transfer* **96**, 139–204 (2005).
15. F.J.M. Harren, G. Cotti, J. Oomens, and S. te Lintel Hekkert, in: *Encyclopedia of Analytical Chemistry*, ed. by R.A. Meyers (John Wiley & Sons Ltd, Chichester, 2000), pp. 2203–2226.